

# Journal Pre-proof

Impact behaviour of MWCNTs reinforced YSZ and Al<sub>2</sub>O<sub>3</sub> ceramic-nanocomposites prepared via vacuum hot-pressing technique

Karthikeyan Ramachandran, Constance L. Gnanasagaran, Ashwath Pazhani, Vishaal Harikrishna Kumar, M. Anthony Xavier, R Ram Subramani, T. Arunkumar

PII: S2238-7854(23)00890-6

DOI: <https://doi.org/10.1016/j.jmrt.2023.04.199>

Reference: JMRTEC 7175

To appear in: *Journal of Materials Research and Technology*

Received Date: 16 March 2023

Accepted Date: 20 April 2023

Please cite this article as: Ramachandran K, Gnanasagaran CL, Pazhani A, Kumar VH, Xavier MA, Subramani RR, Arunkumar T, Impact behaviour of MWCNTs reinforced YSZ and Al<sub>2</sub>O<sub>3</sub> ceramic-nanocomposites prepared via vacuum hot-pressing technique, *Journal of Materials Research and Technology*, <https://doi.org/10.1016/j.jmrt.2023.04.199>.

This is a PDF file of an article that has undergone enhancements after acceptance, such as the addition of a cover page and metadata, and formatting for readability, but it is not yet the definitive version of record. This version will undergo additional copyediting, typesetting and review before it is published in its final form, but we are providing this version to give early visibility of the article. Please note that, during the production process, errors may be discovered which could affect the content, and all legal disclaimers that apply to the journal pertain.

© 2023 Published by Elsevier B.V.



## Impact behaviour of MWCNTs reinforced YSZ and Al<sub>2</sub>O<sub>3</sub> ceramic-nanocomposites prepared via vacuum hot-pressing technique

Karthikeyan Ramachandran<sup>1,2\*</sup>, Constance L Gnanasagaran<sup>1</sup>, Ashwath Pazhani<sup>2</sup>, Vishaal Harikrishna Kumar<sup>3</sup>, M. Anthony Xavior<sup>4</sup>, R Ram Subramani<sup>5,6</sup> and T. Arunkumar<sup>7</sup>

<sup>1</sup>School of Engineering and the Environment, Kingston University, Roehampton Vale Campus, London, United Kingdom SW15 3DW.

<sup>2</sup>School of Mechanical, Aerospace and Automotive, Coventry University, Priory Street, Coventry, United Kingdom CV1 5FB.

<sup>3</sup>Department of Metallurgical Engineering, PSG College of Technology, Coimbatore, India.

<sup>4</sup>School of Mechanical Engineering, Vellore Institute of Technology, Vellore, India.

<sup>5</sup>School of management, Indian Maritime University, Chennai, India.

<sup>6</sup>Kuehne+Nagel International AG Ltd, India.

<sup>7</sup>School of Mechanical Engineering, CMR Institute of Technology, Bangalore, India.

### Abstract

Materials for structure-based aerospace applications are on high demand throughout the globe. Owing to its high strength to weight ratio and high stiffness, composites are potential candidates in aerospace, turbine and military applications. This paper concentrates on the impact behaviour of two nano-ceramic composites - yttria-stabilized zirconia (YSZ) and aluminium oxide (Al<sub>2</sub>O<sub>3</sub>) reinforced with multi-walled carbon nanotubes (MWCNTs) prepared via vacuum hot-pressing at 1600°C with a pressure of 35 MPa at varying MWCNTs contents (1, 3 & 5 wt.%). The composite tiles were examined for impact behaviour using gas gun at different velocities (50, 100 & 200 ms<sup>-1</sup>). The study indicated that the composites with 1 wt.% MWCNTs reinforced YSZ illustrated lower penetration compared to other composites owing to its higher interfacial bonding between MWCNTs and YSZ. On the other hand, alumina reinforced MWCNTs showcased a higher depth of penetration due to weak Van der Waals force of attraction between MWCNTs and alumina. The reinforcement of CNTs upto 3 wt.% worked as threshold for improvement in impact behaviour for ceramics whereas penetration values increase with increase of MWCNTs.

**Keywords:** Ceramics, MWCNTs, Nanocomposites, Densification, Hot-Pressing Technique and Impact behaviour.

**\*Corresponding Author 1:** Constance L Gnanasagaran

**Email:** constance.g@kingston.ac.uk

**\*Corresponding Author 2:** Karthikeyan Ramachandran

**Email:** K1825123@kingston.ac.uk

## Introduction

Engineering ceramics and its composites play an essential role in structural and high temperature applications with potential utilisation in aerospace, manufacturing and military sectors owing to their excellent thermal and corrosion resistance, and their unique optical and electrical properties compared to metallic materials [1, 2]. Regardless of its superior properties such as enhanced thermal and chemical stability at lower density, the use of ceramics in structural applications are limited due to their brittle behaviour [3, 4]. Among various advanced ceramics, alumina and zirconia have been the most popular and are being utilized in various engineering applications due to their excellent physical and thermo-mechanical properties making them exceptional candidates for barrier coatings, water filtrations and other aerospace applications [5, 6, 7]. For the past few decades, there have been progressive and significant research towards improving the thermal and mechanical properties of alumina by reinforcing them with different ceramics including zirconia, mullite and silicon carbide [8, 9, 10]. Zirconia, also a premier biomaterial, have also been studied with reinforcement of different ceramics to improve its mechanical properties in biomedical applications [11, 12]. For example, Orange *et al.* reported that zirconia/mullite composite prepared through dispersion of zirconia particles improved the fracture toughness up to  $5.25 \text{ MPa}\cdot\text{m}^{0.5}$  making them a favourable candidate for orthopaedic load-bearing applications [13].

Over the past few decades, metal alloys like high hardness steel have been the go-to material when it comes to aerospace applications and other structural applications [14]. However, the main disadvantage of materials like these is the heavy weight it possesses, which is a threat especially to the transportation industries as it directly links to high consumption of fuel. Also, metal production alone consumes around 10% of all global energy, making it a significant driver of climate change and other concerns about sustainability [1, 15]. This increased the demand for lightweight materials industrywide and created plenty of opportunities for alternative material research with lower density and higher strength [16, 15]. Hence, due to the superior properties of ceramics and the capability to honour structural integrity at myriad of conditions, they have become key materials for research towards lightweight material applications. However, low fracture toughness of ceramics makes them susceptible to fracture when subjected to higher stresses. Thus, the requirement for reinforcement led to the genesis of composites. Although various reinforcements have supported to enhance the fracture toughness of ceramics, there is still a huge need for improvement as there have been contradictions on the properties of the impact behaviour of the ceramic composites on micro-materials scale [17, 18, 19]. Therefore, many researchers have moved towards new approach

of reinforcing nano-scaled materials such as graphene and carbon nanotubes (CNTs) as well as boron nanotubes into ceramic matrix systems which have proven to be some of the most appropriate reinforcements for nanocomposites [20, 21, 22, 23, 24]. Previous reports on reinforcing MWCNTs with SiC and YSZ for barrier coatings resulted in increased mechanical and thermal properties of ceramic composites up to certain threshold limits [2, 25, 22]. This study will focus on impact performance of hot-pressed multi-walled carbon nanotubes (MWCNTs) reinforced zirconia and alumina at varying percentage (1, 3 & 5 wt.%) prepared via improvised colloidal route and fabricated through hot pressing in vacuum environment.

## Materials and Methods

### *Materials*

Commercially available aluminium oxide ( $\text{Al}_2\text{O}_3$ ) with particle size of ~20-30 nm and purity over ~99% were attained from SRL Pvt. Ltd., Chennai and 3% yttria stabilized zirconia (YSZ) was attained from MK industries, Canada with purity of ~99% and ~50 nm particle size. The MWCNTs was synthesised through thermo-catalytic chemical vapour deposition (TC-CVD) with purity ~97% and size ranging from 20-30 nm as reported in our previous work [26]. The microstructural observation of prepared MWCNTs is illustrated in Figure 1.

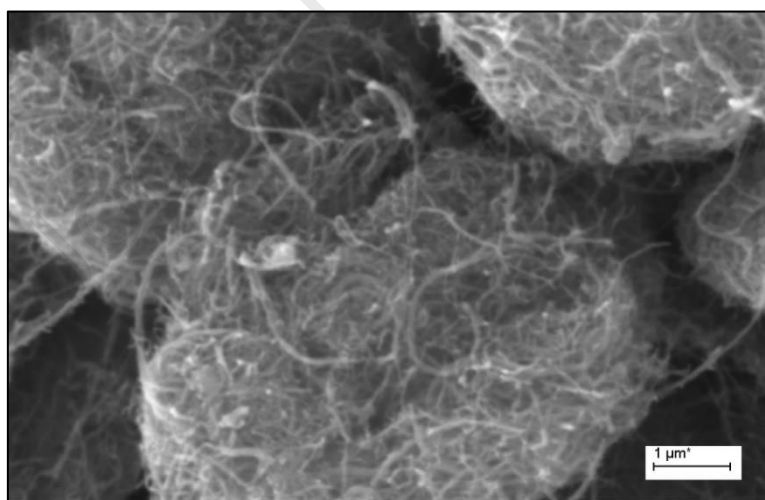


**Figure 1. SE microstructure of MWCNTs cluster prepared via TCCVD technique**

### *Powder Preparation & Fabrication*

Improvised colloidal route was utilised to prepare nanocomposites of  $\text{Al}_2\text{O}_3$  and YSZ reinforced with synthesised MWCNTs as reported in our previous studies [25, 22]. The MWCNTs were dispersed into a mixture of 3:2 ethanol and water medium with a dispersing agent 0.5 wt.% sodium hexametaphosphate and ultrasonicated using a probe-ultrasonicator (PR600MP) at 50 KHz frequency for 20 min. The attained solution was vigorously stirred using

a magnetic stirrer and then ball milled with help of agate balls and container at 300 rpm for 5 h with 5 min rest every 30 min. The milled semi-solid solution was dried using rotary evaporator for 12 h at 100°C and attained powder was crushed and sieved. The prepared composites powders were pressed into composite tiles of 100 mm × 100 mm × t (where t = 5, 7.5 & 10 mm) using vacuum hot-press technique at 1600°C with heating rate of 200°C/min under the pressure of 30 MPa with argon as inert gas and cooling rate of 100°C/min as illustrated in Fig. 2. The dwell time of the composites prepared were dependent on the densification cycle of the composites. The composition of prepared composites tiles is provided in Table. 1.

**Table 1. Composition of composite tiles with respect to MWCNTs content**

Ceramics	Composites Nomenclature	Ceramic Percentage (wt.%)	MWCNTs percentage (wt.%)
Al <sub>2</sub> O <sub>3</sub>	AC0	100	0
	AC1	99	1
	AC3	97	3
	AC5	95	5
YSZ	YC0	100	0
	YC1	99	1
	YC3	97	3
	YC5	95	5

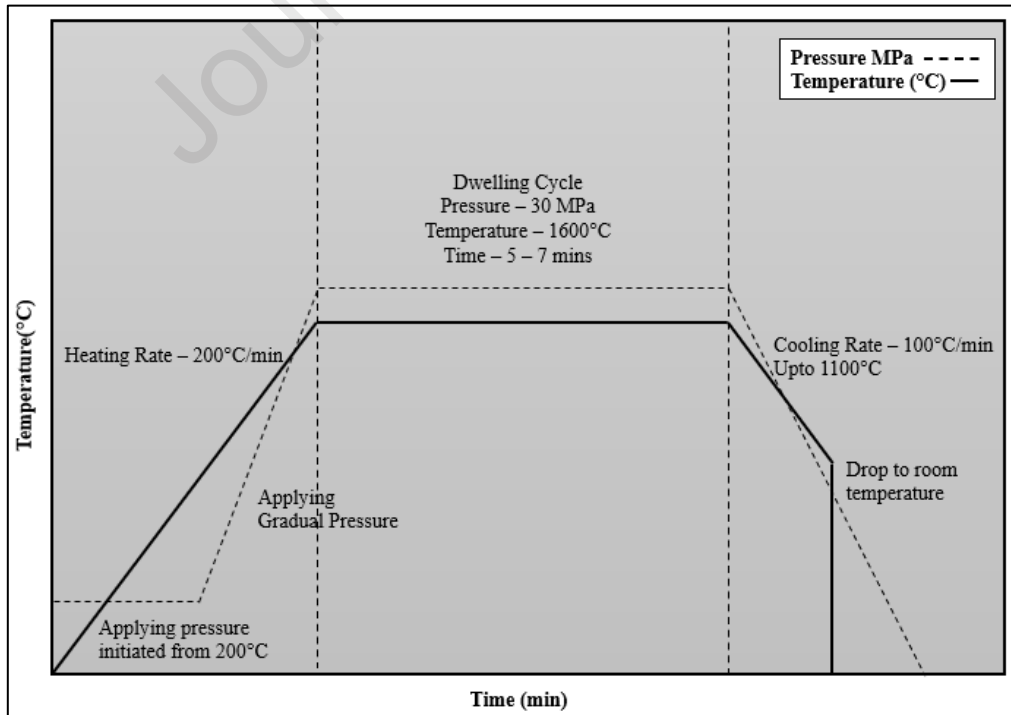


**Figure 2. Temperature profile of ceramics and composites tiles through vacuum hot-pressing technique in vacuum environment in presence of Ar atmosphere**

### *Characterisation & Testing Method*

The hot-pressed samples were characterized through scanning electron microscopy (Zeiss Supra 55) along with simultaneous quantitative analysis (EDS). For SEM studies, samples were coated with Au/Pt nanoparticles through sputter coating. The relative density of the composites was measured through Archimedes technique with water as a immersive medium. An average of three composites relative density was measure and reported. Also, impact study which was carried out using pneumatic piston operated gas gun at different velocities (50, 100 & 200 ms<sup>-1</sup>). The penetration bullets were made by casting technique using Titanium alloy and further heat-treating the composites to attain a bullet of weight of 5.2 g and diameter of 7.62 mm. The penetration bullet was cast with a hemispherical nose and with a total length of 18.50 mm. The composite tiles were supported using a hard steel frame and an aluminium alloy based back plate.

## **Results and Discussion**

### *Densification behaviour*

The relative density of Al<sub>2</sub>O<sub>3</sub> and YSZ ceramics and its composites tiles with respect to MWCNTs content is illustrated in Fig. 3. The relative density of alumina ceramic tiles was over ~99% whereas with increase in MWCNTs content, the relative density degraded to ~94%. Likewise, YSZ showed a density of 99% for monolithic, which also degraded to ~96% with increase in MWCNTs content. The higher densities of the composites (>90%) could be due to joule's heating attained from the hot pressing of the ceramics and MWCNTs particles. The higher thermal conductivity of MWCNTs supported in enhancing the joule's heating between the particles leading to higher density. From Fig. 2, it could be observed that relative densities degraded with increase in MWCNTs content which was similar to previously reported research on spark plasma sintered SiC and YSZ composites [25, 22]. This decrease in relative density could be attributed towards agglomeration of the CNTs which could have led to an increase in the open pore networks, resulting in the drop in densities. This formation of agglomeration throughout the samples could have led to a reduction in joule heating between the nanoparticles by providing low resistance during sintering [27]. The relative densities of alumina composites demonstrated more degradation compared to YSZ and its composites, owing to its pinning effects of MWCNTs which inhibits grain growth and restricting densification however, the higher stability of YSZ makes it hard to pin the grain growth [28].

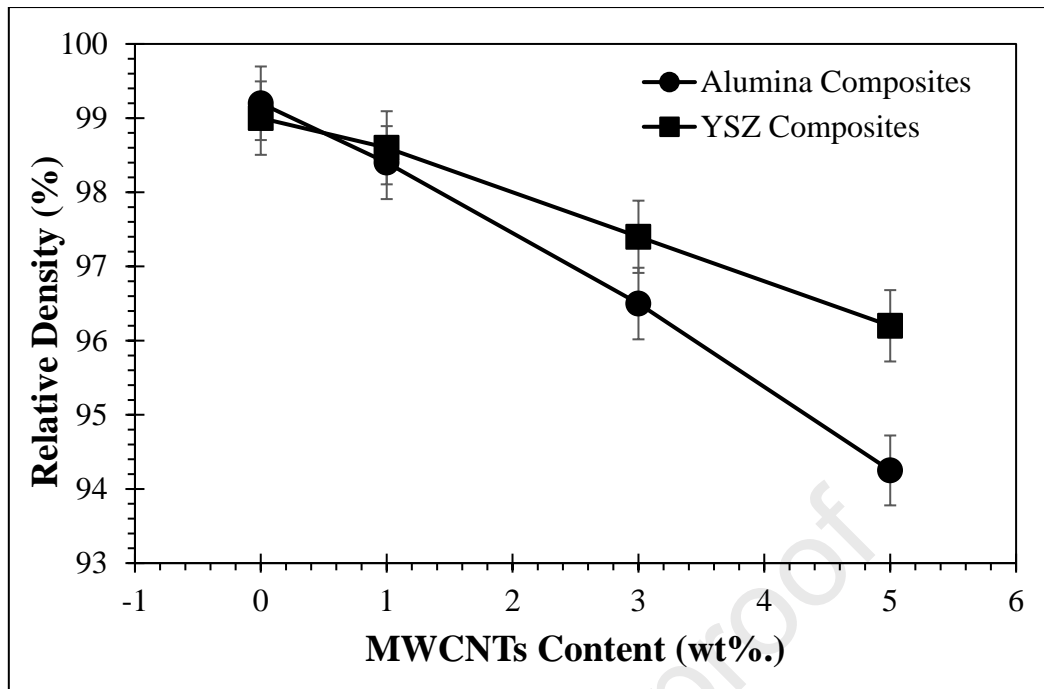


**Figure 3. Relative Densities of nanocomposites with respect to MWCNTs content.**

Scanning electron image of  $\text{Al}_2\text{O}_3$  and YSZ ceramic tiles reinforced with 1 wt.% MWCNTs is illustrated in Fig. 4. From Fig. 4(a), it is visible that surface of alumina reinforced with 1 wt.% indicated fine distribution of alumina throughout the surface with small particles agglomeration on the surfaces. This agglomeration on the surface is due to MWCNTs while sintering. Elemental distribution (EDS) on the surfaces of agglomeration area revealed high traces of carbon content (74%) and small traces of aluminium (9.43%) and oxygen (10.42%), indicating alumina traces. The mixed traces of Al, O and C support the homogenous mixing on the MWCNTs and  $\text{Al}_2\text{O}_3$ . The closer observation (Fig. 4(a) - Right) showcases small pores on the surfaces which could have been the result of drop in relative density. The surface morphology of AC1 exhibits closed and open pores with closely packed particles supporting high interfacial bonding on the surfaces of the material. On the other hand, YC1 (Fig. 4(b)) showcases plenty of open pores throughout the surfaces. Even with many open pores, the YC1 showcased a higher relative density owing to the homogeneous distribution and strong Van der Waals force of attraction among CNTs which holds the YSZ and MWCNTs in place [3].



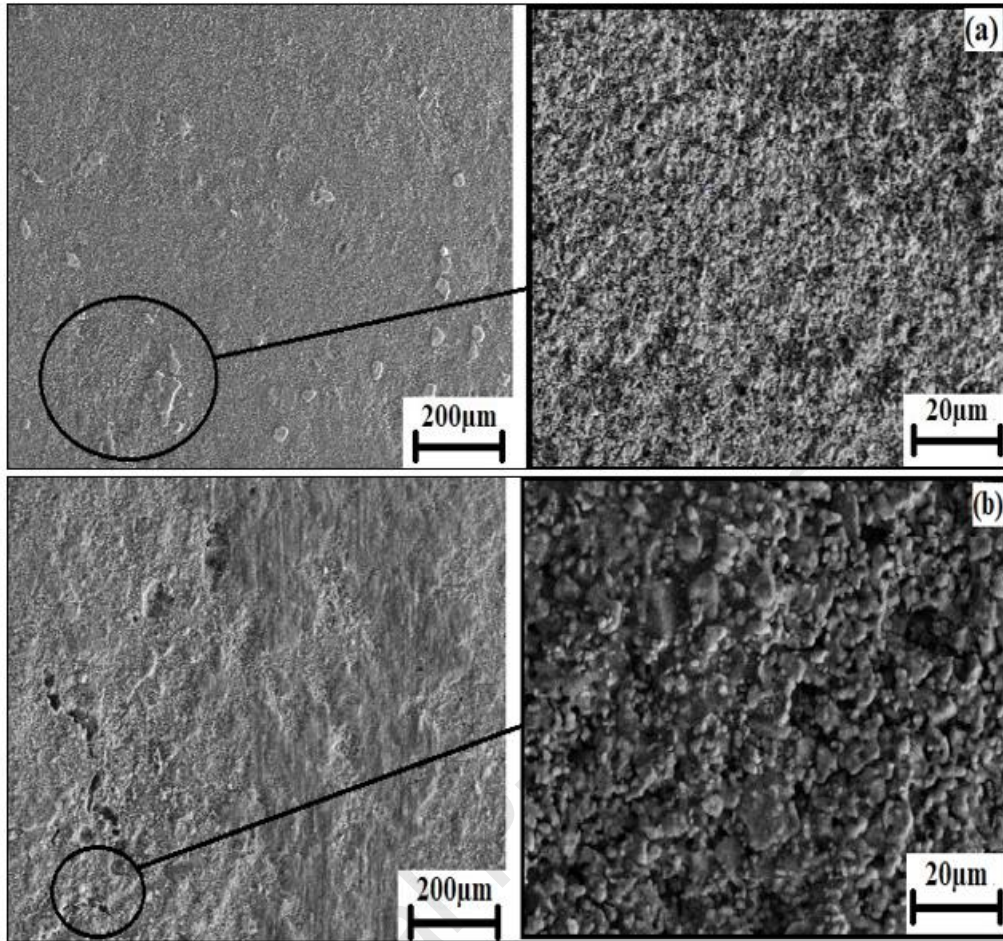


**Figure 4. Scanning electron microscopic observation of (a)  $\text{Al}_2\text{O}_3$  reinforced 1 wt.% MWCNTs and (b) YSZ reinforced 1 wt.% MWCNTs**

**Table 2. Porosity of ceramics and nanocomposites calculated through linear intercept technique**

<b>Composites Labels</b>	<b>Largest void span (nm)</b>	<b>Largest void area (<math>\text{nm}^2</math>)</b>	<b>Porosity (%)</b>	<b>Analysed average particle size (nm)</b>
AC0	4.22	44.26	0.49	17
AC1	4.98	49.37	1.28	16
AC3	5.29	54.67	2.63	16
AC5	5.96	60.42	3.95	16
AC0	3.16	28.95	0.38	38
YC1	3.76	30.26	0.82	36
YC3	4.10	33.95	1.46	37
YC5	4.76	38.43	2.98	38

The EDS on the region closer to the open pores showcased traces of carbon which were embedded onto the YSZ particles. Further surface morphology of YSZ showed larger grain size which were determined to be about  $\sim 38$  nm through linear interpretation technique using ImageJ software, which was higher than that of alumina ( $\sim 17$  nm). The reduction in the grain size could have been due to the ball milling process with agate balls which could have reduced



the size of particles. The porosity of the composites was also calculated and reported in Table 2 which were determined through line intercept technique. It can be observed that with increase in the MWCNTs content, there was an extensive increase in porosity value throughout the composite. This could have been due to the reduction in the particle size which inhibited the Van der Waals attraction force of the CNTs. The elemental distribution of 3 wt.% MWCNTs reinforced alumina and YSZ is illustrated in Fig. 5 showcased homogenous distribution of carbon elements onto the surfaces of YSZ and alumina. The presence of yttria in Fig. 5(a) supports the case of stabilisation of  $ZrO_2$  through 3 mol% of yttria and presence of carbon traces supports the MWCNTs reincorporation on the matrix. Likewise, the traces of the carbon in alumina composite also supported MWCNTs reinforcement.

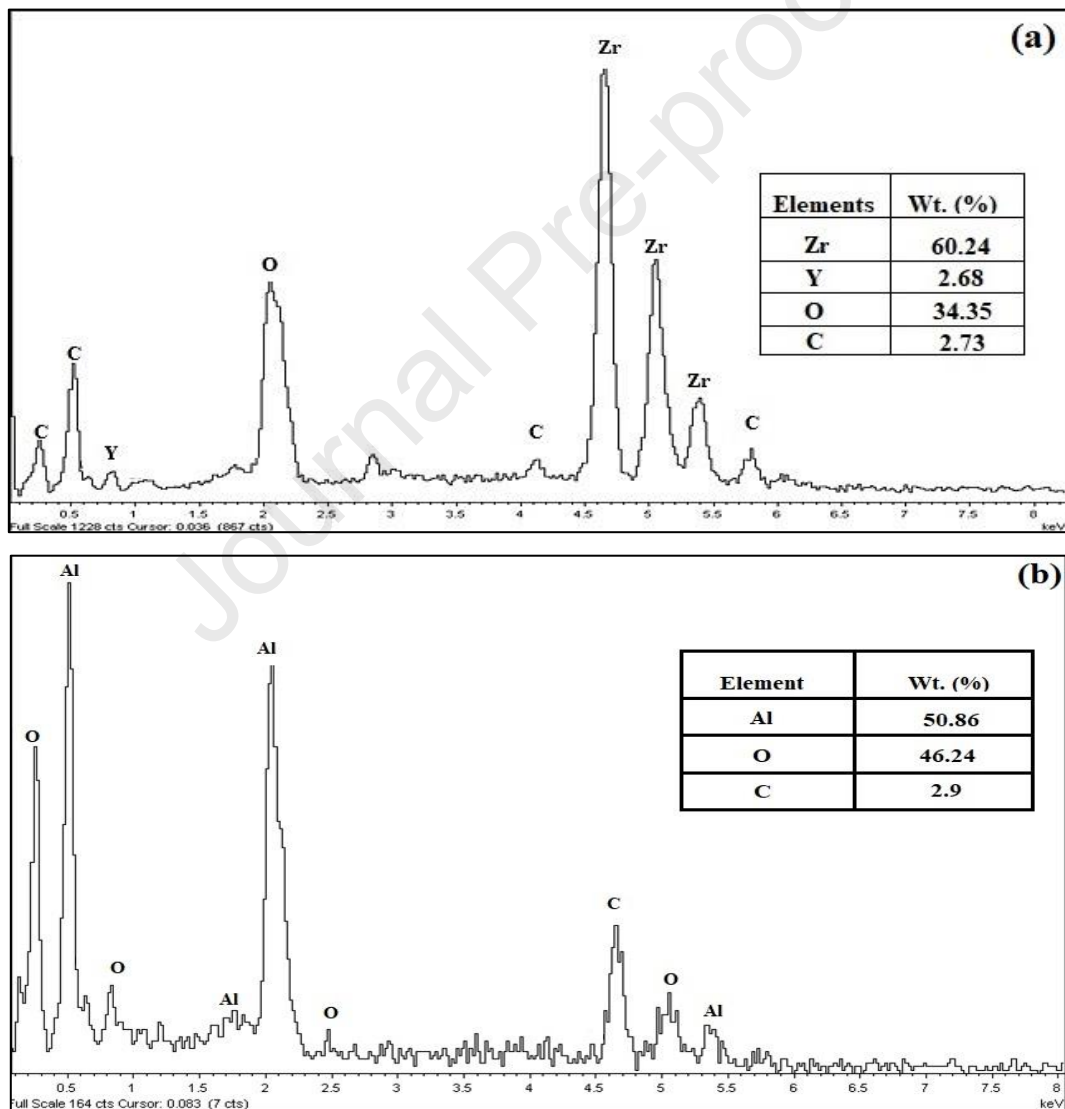


**Figure 5. Elemental distribution plots of 3 wt.% MWCNTS reincorporated (a)YSZ and (b)alumina composites.**

*Effect of composite tile thickness*

The monolithic ceramics and its nanocomposites tiles were evaluated for their mass efficiency ( $E_m$ ) according to their thickness. Mass efficiency ( $E_m$ ) was calculated based on Eq. (1) where  $\rho_A$  and  $\rho_C$  are densities of aluminium alloy block and composites,  $t_c$  is thickness of tiles and  $P_\infty$  represents the depth of penetration at different ranges and  $P_r$  represents the residual DOP of the backing plates respectively. The Eq. (1) supports the semi-infinite target configuration owing to the thin composite tile thickness and the utilisation of backing plate made from heat treated aluminium alloy block [29].

$$E_m = \frac{[\rho_A \times P_\infty]}{[(t_c \times \rho_C) + (\rho_A \times P_r)]} \quad (1)$$

Figure 6 plots the calculated mass efficiency with respect to thickness of monolithic ceramic and composite tiles. From the plot, it is visible that mass efficiency of the monolithic ceramics and its composites enhances with respect to thickness. Likewise, composites also indicated enhancement in the thickness with certain MWCNTs reinforcements content. The monolithic alumina showed a mass efficiency of ~0.84 which increased upto ~1.98 with increase in thickness. These values are slightly higher than previously reported data where alumina were produced using rapid prototyping [29].

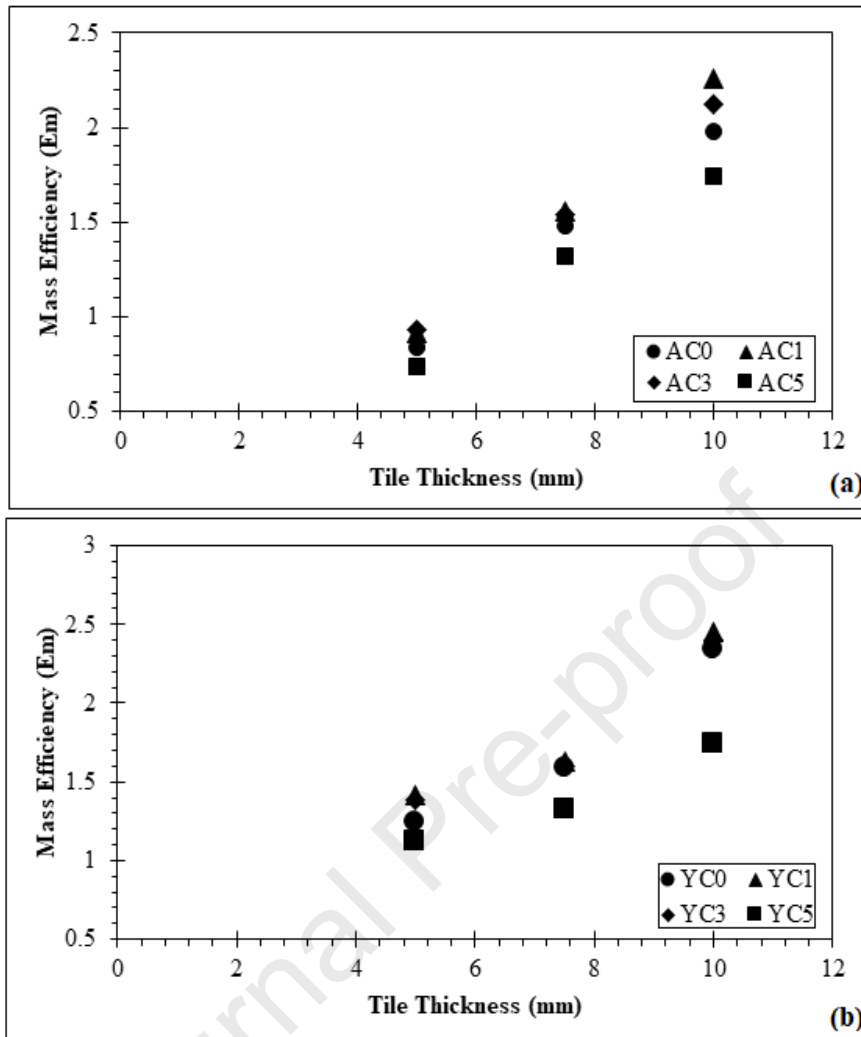


**Figure 6. Mass efficiency ( $E_m$ ) for (a) alumina ceramics and its nanocomposites and (b) YSZ ceramics and its nanocomposites**

This could have been due to the higher relative density of monolithic alumina which was fabricated through vacuum hot-pressing technique. Alumina reinforced ceramic nanocomposites indicated enhanced mass efficiency compared to monolithic alumina by ~7% for 1 wt.% MWCNTs and ~12% for 3 wt.% MWCNTs. This increase was in relationship with enhancement in the fracture toughness behaviour of the CNTs reinforced alumina composites where the fracture bridging and fiber pull-out mechanisms were operational. Further, when load was applied on the surfaces, CNTs untangled from their spring structure which enhances the pull-out mechanism between CNTs and ceramics particles enhancing its already high fracture toughness [3]. However, AC5 showed the least mass efficiency compared to other alumina and its composites. This could be due to the high number of open pores throughout the surfaces of the composites. However, YSZ and its CNT reinforced composites indicated higher mass efficiency compared to the alumina owing to their structural stability due to

enhanced fracture mechanisms [30]. Further, YSZ nanocomposites showcased the same trend of gain in mass efficiency until 3 wt.% MWCNTs which further reduced with further increase in MWCNTs content. Although, unlike alumina composites, values of YSZ indicated close values to monolithic YSZ compared to alumina. The higher amount of MWCNTs content led to agglomeration on the composites leading to high number of pores which reduce the hardness and fracture toughness of composites, leading to failure [25].

#### *Effect of Impact Velocity*

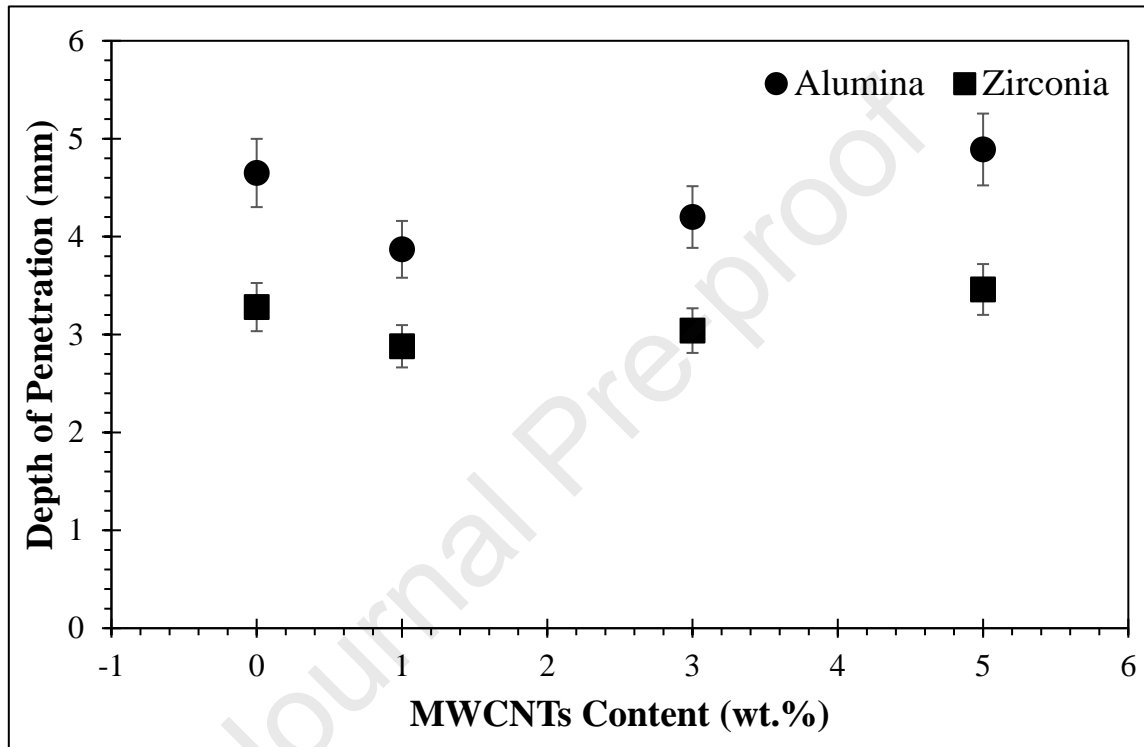


**Figure 7. Depth of penetration at velocity of  $50 \text{ ms}^{-1}$  with respect to MWCNTs content (wt.%)**

The impact study on the ceramics and its reinforced composites were conducted at 50 m/s velocity and depth of penetration (DOP) of projectile was measured using optical microscope and plotted in Figure 7. From Figure 7, it is visible that ceramics reinforced with the 1 wt.% MWCNTs i.e., AC1 and YC1 displayed lower penetration compared to monolithic and other composites. Likewise, AC3 and YC3 represented lower DOP compared to monolithic ceramics but higher than AC1 and YC3. The reduction on AC1, AC3, YC1 and YC3 composites is due to MWCNT incorporation which enhanced the interfacial bonding between CNTs and the ceramics Van der Waals force which increases the interaction [25, 22]. The strong interfacial bonding between the CNTs and ceramics could have been due to the bridging of MWCNT fibers with the ceramic particles throughout the surfaces [3]. On the other hand, higher

MWCNTs percentage onto ceramics led to a higher DOP compared to monolithic ceramics showcasing damages leading to failure which was the case of AC5 and YC5. This could be a result of agglomeration of MWCNTs on the composite surface, resulting in a lowered hardness and fracture toughness and thus leading to failure of the composite.

**Table 3. Depth of penetration on composites of 10 mm tile thickness at 100 and 200 m/s**

MWCNTs Content (wt.%)	Alumina		Zirconia	
	100 m/s	200 m/s	100 m/s	200 m/s
0	5.96	7.89	4.18	7.05
1	4.16	8.65	3.98	6.49
3	6.25	9.86	5.86	8.94
5	8.2	-	7.27	-

Table 3 reports the DOP for the MWCNTs reinforced composites at 100 and 200 m/s impact velocity. From Table 3, it could be stated that both alumina and zirconia-based ceramics and its composites were able to withstand 100 m/s impact velocity. However, at 200 m/s, 5 wt.% MWCNTs reinforced composites failed completely. This showcases that velocity of projectile, and its relative density affected the composite tile with respect to its hardness and fracture behaviour. The drop in the fracture toughness with respect to MWCNTs reinforcements could be due to agglomeration of MWCNTs on the surfaces due to weak Van der Waals force of attraction between ceramic and MWCNTs. This agglomeration of MWCNTs led to reducing on the sintering effect of the composites [23, 24].

Figure 8 represents the surface impact mechanics schematic view on the impact area and its microstructures of the AC3 and YC3 samples. From Fig. 8, it is evident that the impact of Ti bullet caused an initial shearing effect to initiate the penetration. Comparing the AC3 and YC3, YC3 exhibited reduced DOP compared to AC3 which is reported in Table 3. This phenomenon could be due to two significant factors like damping effect and compressive effect created post impact. From Fig. 8 FESEM, it is clearly visible that the impact created an uniform compressive force in the circumference of impact zone which led to drop in the pinning effect between the MWCNTs and ceramics. This drop in pinning effect facilitated effective load transferring capability of the composites resulting in lower DOP and also leaving traces of bow-back resistance on the impact region as highlighted in Fig. 8 [31]. This sort of impact mechanism was not observed for AC3 due to the lower relative density which resulted in high DOP. It could be presumed by observation that the shear between the Ti bullet to the ceramic to be ~40% for AC3 and ~60% for YSZ. This shear could also have been due to the abrasive

nature of the ceramics which are being created from the interaction between bullet and the ceramic composite.

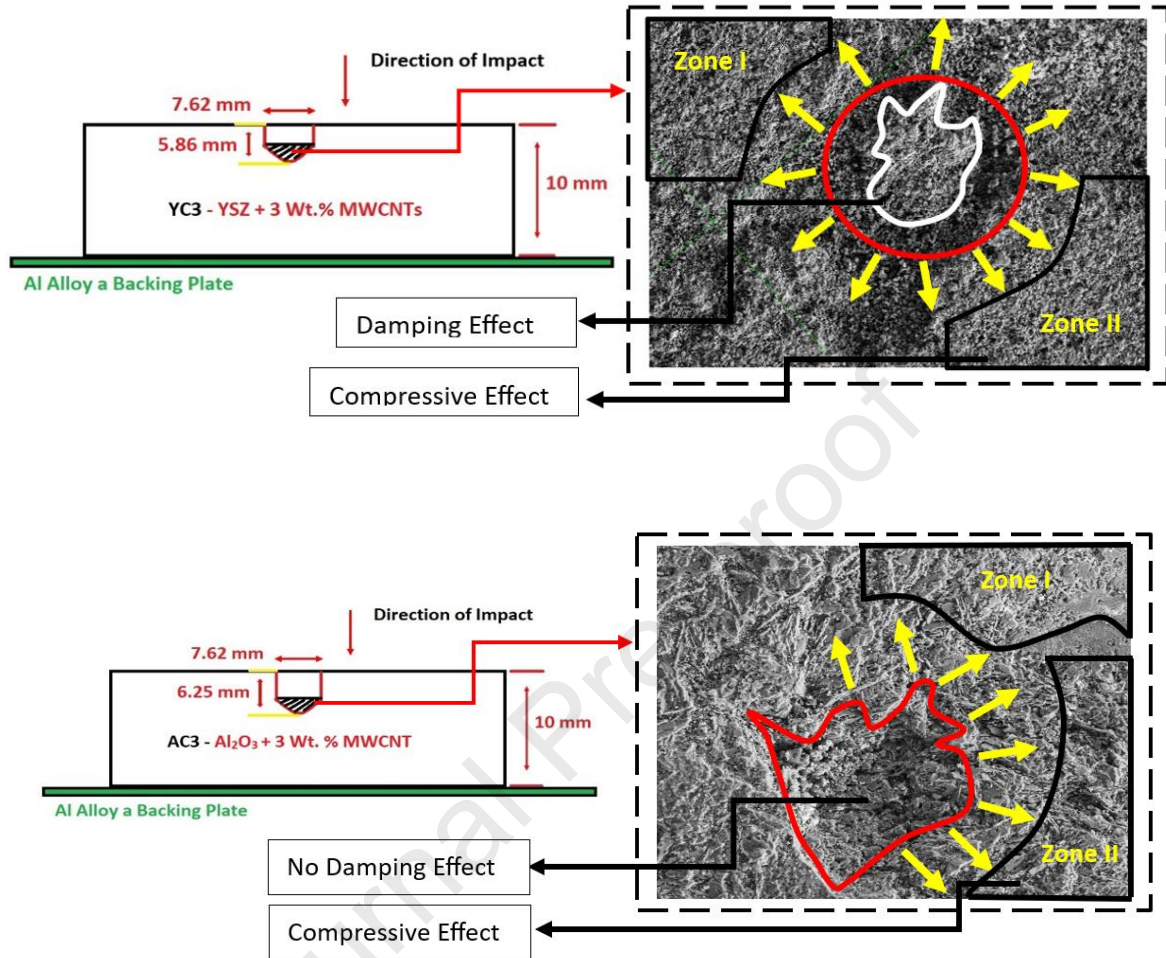


**Figure 8. Impact surface mechanics and microstructure of (a) YC3 and (b) AC3**

## Conclusion

The impact behaviour of the monolithic alumina, YSZ and its MWCNTs reinforced composites against a Ti-alloy projectile has been reported in this study. The results indicated that with an increase in MWCNTs content, the depth of penetration into the composites increased with 3 wt.% MWCNTs reinforcement acting as a threshold limit. The reduction in the penetration depth at 1 wt.% reinforcement in alumina and YSZ was attributed towards the enhanced interfacial bonding and Van der Waals forces of attraction between the ceramic and MWCNTs. On contrary, increase in the DOP upon increase in the content of MWCNTs is imputed to the agglomeration of CNTs during sintering that leads to a lower hardness and fracture toughness owing to formation of open pores throughout the surfaces. The study also showed that YSZ and its composites consistently exhibited lower DOP than alumina and its composites owing



to its higher relative density. In spite of their low weight and density, the alumina based ceramic composites have typical shortcomings that might need consideration while designing for aerospace structural systems. It was also observed that with a decrease in relative density of the tiles, the DOP increased, implying an inverse relation between densification and penetration depth. Further, to understand the impact behaviour of the ceramic nanocomposites in depth, extensive research is required with focus towards sintering, high velocity impacts and projectile dimensions.

## References

- [1] C. Gnanasagaran, K. Ramachandran, S. Ramesh, S. Ubenthiran and N. Jamadon, "Effect of co-doping manganese oxide and titania on sintering behaviour and mechanical properties of alumina," *Ceramics International*, vol. 49, no. 3, pp. 5110-5118, 2023.
- [2] K. Ramachandran, V. Boopalan, J. Bear and R. Subramani, "Multi-walled carbon nanotubes (MWCNTs)-reinforced ceramic nanocomposites for aerospace applications: a review," *Journal of Materials Science*, vol. 57, pp. 3923-3953, 2022.
- [3] K. Ramachandran, R. Subramani, T. Arunkumar and V. Boopalan, "Mechanical and thermal properties of spark plasma sintered Alumina-MWCNTs nanocomposites prepared via improvised colloidal route," *Materials Chemistry and Physics*, vol. 272, no. 125034, pp. 1-9, 2021.
- [4] G. Zhan and A. Mukherjee, "Carbon nanotube reinforced alumina-based ceramics with novel mechanical, electrical, and thermal properties," *International Journal of applied ceramic Technology*, vol. 1, no. 2, pp. 161-171, 2005.
- [5] H. Fang, J. Gao, H. Wang and C. Chen, "Hydrophobic porous alumina hollow fiber for water desalination via membrane distillation process," *Journal of Membrane Science*, Vols. 403-404, pp. 41-46, 2012.
- [6] K. Mondal, L. III, C. Downey and I. Rooyen, "Thermal barrier coatings overview: design, manufacturing, and applications in high-temperature industries," *Industrial & Engineering Chemistry Research*, vol. 60, no. 17, pp. 6061-6077, 2021.
- [7] C. Zuccarini, K. Ramachandran, S. Russo, Y. Jayakody and D. Jayasselam, "Mathematical modeling and simulation of porosity on thermomechanical properties of UHTCs under hypersonic conditions," *International Journal of Ceramic Engineering & Science*, 2022.
- [8] P. Bercher and G. Wei, "Toughening behavior in SiC-whisker-reinforced alumina," *Journal of the American Ceramic Society*, vol. 67, no. 12, pp. C267-269, 1984.
- [9] K. Takahashi, M. Yokouchi, S. Lee and K. Ando, "Crack-healing behavior of Al<sub>2</sub>O<sub>3</sub> toughened by SiC whiskers," *Journal of the American Ceramic Society*, vol. 86, no. 12, pp. 2143-2147, 2003.

- [10] J. Silvestre, N. Silvestre and J. d. Brito, "An overview on the improvement of mechanical properties of ceramics nanocomposites," *Journal of Nanomaterials*, pp. 1687-4110, 2015.
- [11] C. Gautam, J. Joyner, A. Gautam, J. Rao and R. Vajtai, "Zirconia based dental ceramics: structure, mechanical properties, biocompatibility and applications," *Dalton Transactions*, vol. 45, pp. 19194-19215, 2016.
- [12] M. Aboushelib, J. Matinlinna, Z. Salameh and H. Ounsi, "Innovations in bonding to zirconia-based materials: Part I," *Dental Materials*, vol. 24, no. 9, pp. 1268-1272, 2008.
- [13] G. Orange, G. Fantozzi, F. Cambier, C. Leblud, M. Anseau and A. Leriche, "High temperature mechanical properties of reaction-sintered mullite/zirconia and mullite/alumina/zirconia composites," *Journal of Materials Science*, vol. 20, pp. 2533-2540, 1985.
- [14] S. Ryan, H. Li, M. Edgerton, D. Gallardy and S. Cimpoeru, "The ballistic performance of an ultra-high hardness armour steel: An experimental investigation," *International Journal of Impact Engineering*, vol. 94, pp. 60-73, 2016.
- [15] I. G. Crouch, "Body armour – New materials, new systems," *Defence Technology*, vol. 15, no. 3, pp. 241-253, 2019.
- [16] A. E. Medvedev, T. Maconachie, M. Leary, M. Qian and M. Brandt, "Perspectives on additive manufacturing for dynamic impact applications," *Materials & Design*, vol. 221, no. 110693, pp. 1-23, 2022.
- [17] G. A. Gogotsi, "Fracture toughness of ceramics and ceramic composites," *Ceramics International*, vol. 29, no. 7, pp. 777-784, 2003.
- [18] T. Nose and T. Fujii, "Evaluation of fracture toughness for ceramic materials by a single-edge-precracked-beam method," *Journal of the American Ceramic Society*, vol. 71, no. 5, pp. 328-333, 1988.
- [19] R. Beaumont, "An investigation into the relationship between thermal shock resistance and ballistic performance of ceramic materials," University of Surrey, Surrey, 2016.
- [20] C. Gao, P. Feng, S. Peng and C. Shuai, "Carbon nanotube, graphene and boron nitride nanotube reinforced bioactive ceramics for bone repair," *Acta Biomaterialia*, vol. 61, pp. 1-20, 2017.
- [21] X. Mu, H. Zhang, H. Cai, Q. Fan, Z. Zhang, Y. Wu, Z. Fu and D. Yu, "Microstructure evolution and superior tensile properties of low content graphene nanoplatelets reinforced pure Ti matrix composites," *Materials Science and Engineering: A*, vol. 687, pp. 164-174, 2017.
- [22] T. Arunkumar, R. Karthikeyan, R. Subramani, M. Anish, J. Theerthagiri, R. Boddula and J. Madhavan, "Effect of MWCNTs on improvement of fracture toughness of spark plasma sintered SiC nano-composites," *Current Analytical Chemistry*, vol. 16, no. 1, 2020.
- [23] N. Sharma, A. Syed, B. Ray, S. Yadav and K. Briswas, "Alumina–MWCNT composites: microstructural characterization and mechanical properties," *Journal of Asian Ceramic Societies*, vol. 7, pp. 1-19, 2019.
- [24] S. Cho, J. Kim, S. Lee, M. Choi, D. Kim, I. Jo, H. Kwon and Y. Kim, "Fabrication of functionally graded hydroxyapatite and structurally graded porous hydroxyapatite by

- using multi-walled carbon nanotubes," *Composites Part A: Applied Science and Manufacturing*, vol. 139, no. 106139, pp. 1-11, 2020.
- [25] T. Arunkumar, G. Anand, R. Subbiah, R. Karthikeyan and J. Jeevahan, "Effect of multiwalled carbon nanotubes on improvement of fracture toughness of spark-plasma-sintered Yttria-stabilized Zirconia nanocomposites," *Journal of Materials Engineering and Performance*, vol. 30, pp. 3925-3933, 2021.
- [26] T. Arunkumar, R. Karthikeyan, R. R. Subramani, K. Viswanathan and M. Anish, "Synthesis and characterisation of multi-walled carbon nanotubes (MWCNTs)," *International Journal of Ambient Energy*, vol. 41, no. 4, pp. 452-456, 2020.
- [27] A. Nisar, S. Ariharan, T. Venkateswaran, N. Sreenivas and K. Balani, "Oxidation studies on TaC based ultra-high temperature ceramic composites under plasma arc jet exposure," *Corrosion Science*, vol. 109, pp. 50-61, 2016.
- [28] S.-L. Shi and J. Liang, "Effect of multiwall carbon nanotubes on electrical and dielectric properties of Yttria-stabilized zirconia ceramic," *Journal of the American Ceramic Society*, vol. 89, no. 11, pp. 3533-3535, 2006.
- [29] G. J. Appleby-Thomas, K. Jaansalu, A. Hameed, J. Painter, J. Shackel and J. Rowley, "A comparison of the ballistic behaviour of conventionally sintered and additively manufactured alumina," *Defence Technology*, vol. 16, no. 2, pp. 275-282, 2020.
- [30] G. Jin, Y. Fang, X. Cui, C. Wang, D. Zhang, X. Wen and Q. Mi, "Effect of YSZ fibers and carbon nanotubes on bonding strength and thermal cycling lifetime of YSZ-La<sub>2</sub>Zr<sub>2</sub>O<sub>7</sub> thermal barrier coatings," *Surface and Coatings Technology*, vol. 397, no. 125986, pp. 1-11, 2020.
- [31] S. Wu, P. Sikdar and G. Bhat, "Recent progress in developing ballistic and anti-impact materials: Nanotechnology and main approaches," *Defence Technology*, 2022.

**Declaration of interests**

The authors declare that they have no known competing financial interests or personal relationships that could have appeared to influence the work reported in this paper.

The authors declare the following financial interests/personal relationships which may be considered as potential competing interests:

Journal Pre-proof